Carbohydrate Polymers 95 (2013) 530–539

Contents lists available at SciVerse ScienceDirect

Carbohydrate Polymers

journal homepage: www.elsevier.com/locate/carbpol

In vivo evaluation of chitosan–PVP–titanium dioxide nanocomposite as wound dressing material

D. Archana [a], Brijesh K. Singh [a], Joydeep Dutta [b], P.K. Dutta [a,*]

[a] Department of Chemistry, Motilal Nehru National Institute of Technology, Allahabad 211004, India
[b] Department of Humanities and Applied Sciences, Institute of Engineering & Technology, ITM University, Uparwara, Raipur 493661, India

ARTICLE INFO

Article history:
Received 13 October 2012
Received in revised form 6 March 2013
Accepted 7 March 2013
Available online 15 March 2013

Keywords:
Chitosan
PVP
Titanium dioxide
In vivo
Wound healing applications

ABSTRACT

In our present study, the blends of chitosan, poly(N-vinylpyrrolidone) (PVP) and titanium dioxide (TiO_2) were investigated by Fourier transform infrared (FTIR) spectroscopy and thermogravimetric analysis (TGA). The size distribution of the TiO_2 nanoparticles was measured using transmission electron microscope and scanning electron microscope. The studies on the mechanical properties of composite material indicate that the addition of TiO_2 nanoparticles increases its strength. The prepared nanocomposite dressing has excellent antimicrobial efficacy and good biocompatibility against NIH3T3 and L929 fibroblast cells. Compared to conventional gauze, soframycin skin ointment and chitosan treated groups, the prepared nano dressing caused an accelerated healing of open excision type wounds in albino rat model. The synergistic effects of nanocomposite dressing material like good antibacterial ability, high swelling properties, high WVTR, excellent hydrophilic nature, biocompatibility, wound appearance and wound closure rate through *in vivo* test makes it a suitable candidate for wound healing applications.

1. Introduction

Wound healing, as a normal biological process in the human body, is achieved through four precisely and highly programmed phases: hemostasis, inflammation, proliferation and remodeling. The main aim of wound healing is a speedy recovery with minimal scarring and maximal function. The selection of materials is very important from wound healing application point of views. Chitosan, a copolymer of glucosamine and N-acetylglucosamine units linked by β-1,4-glycosidic linkages and good biodegradability, nontoxicity, biocompatibility and antifungal activity, and its derivatives have been widely used in the fields of medicine, cosmetics, agriculture, biochemical separation systems, tissue engineering and so on (Archana, Dutta, & Dutta, 2010; Jayakumar, Selvamurugan, Nair, Tokura, & Tamura, 2008; Jia et al., 2011; Leea, Chang, Yang, Chien, & Lai, 2012; Muzzarelli, Greco, Busilacchi, Sollazzo, & Gigante, 2012; Tripathi, Mehrotra, & Dutta, 2009a, 2009b). Chitosan promotes surface induced thrombosis and blood coagulation (Amiji, 1995) and accelerates coagulation *in vivo* by influencing the activation of platelets (Muzzarelli et al., 2007).

The N-acetyl glucosamine (NAG) present in chitin and chitosan is a major component of dermal tissue which is essential for repair of scar tissues (Singh & Ray, 2000). Chitosan's positive surface charge enables it to effectively support cell growth (Kean, Roth, & Thanou, 2005). Chitosan has several advantages over other type of disinfectants because it possesses a higher antibacterial activity, a broader spectrum of activity, a higher killing rate and a lower toxicity toward mammalian cells. Its antibacterial and acceleration of wounds makes it as wound healing material in various forms like beads, powders, gels, sponges, tubes, fibers and films (Li, Kong, et al., 2012; Li, Nan, Li, Zhang, & Chen, 2012; Muzzarelli, 2009; Wang, Liu, Li, Ren, & Ji, 2012; Wang, Wang, Li, Ren, & Ji, 2012; Wang, Zhu, Xue, & Wu, 2012).

PVP, a synthetic polymer, has good biocompatibility and for many years has been applied as a biomaterial or additive to drug compositions, *e.g.* as a blood plasma expander (Zileinski & Acbischer, 1994) and as vitreous humor substitute (Altemeier et al., 1954). Under action of ionizing radiation, PVP undergoes crosslinking and lead to the formation of PVP hydrogel having excellent transparency and biocompatibility. It has been used as a main component of temporary skin covers or wound dressing. However, the hydrogel of PVP itself is of limited applicability because of its poor mechanical properties. So, a series of PVP hydrogels prepared by PVP blends play a significant role as biomedical materials. The miscibility of chitosan and PVP in the films has been reported and is considered that carbonyl groups in the pyrrolidone rings of PVP interact with amino and hydroxyl groups present in chitosan by forming hydrogen bonding and produces material of a novel characteristics (Hong et al., 1998). Since synthetic polymers are available at a lower price than biopolymer chitosan, substitution of chitosan by these synthetic polymers could reduce the price of chitosan-based films with safe effect on their functionality.

* Corresponding author. Tel.: +91 532 2271272; fax: +91 532 2545341.
E-mail address: pkd_437@yahoo.com (P.K. Dutta).

0144-8617/$ – see front matter © 2013 Elsevier Ltd. All rights reserved.
http://dx.doi.org/10.1016/j.carbpol.2013.03.034

Nanosized titanium dioxide (TiO_2) particles occupy a special place due to its favorable biological effects and high corrosion resistance. TiO_2 is also widely used as food and pharmaceutical additive, as well as white pigment in the paper industry and in cosmetic products. The TiO_2 nanotube films have been extensively explored as adhesion and growth support platforms for bone and stem cells for the prevention of bacterial adhesion, drug delivery and enhancing blood clotting for control of hemorrhage (Brammer, Oh, Gallagher, & Jin, 2008; Peng, Eltgroth, LaTempa, Grimes, & Desai, 2009; Tang et al., 2009). Nanoparticles of titanium dioxide are used in cosmetics, filters that exhibit strong germicidal properties and remove odors, and in conjunction with silver as an antimicrobial agent. It is considered non-toxic and has been approved by the American Food and Drug Administration (FDA) for use in human food, drugs, cosmetics and food contact materials (Wist, Sanabria, Dierolf, Torres, & Pulgarin, 2004). The nanoparticles provide a slow release of titanium ions that have wound healing and antimicrobial properties. The titanium ions released from nanoparticle inhibits microbial proliferation and hence it accelerates wound healing (Grassian, Oshaughnessy, Adamcakova-Dodd, Pettibone, & Thorne, 2007). Nontoxicity studies examining the effects of TiO_2 have shown induction of inflammatory responses, cytotoxicity and reactive oxygen species (ROS) formation in a variety of cell types and tissues (Ian, Su, & Tan, 2011; Sayes et al., 2006). CS–TiO_2 complex film was reported due to their good surface properties and bactericidal activities (Han, Su, & Tan, 2006; Lieder et al., 2012; Peng et al., 2008). In a very recent study, Chen et al. shown that polyurethane based TiO_2 membrane as an excellent wound dressing material (Chen, Yan, Yuan, Zhang, & Fan, 2011). Our present study is much more effective wound healing substance because the basic material is natural biopolymer.

The individual features of each chitosan, PVP and TiO_2 nanoparticle have inspired us the feasibility of combining all those to make an effective material for wound healing application. The water/wound secretions may trigger the nanoparticle's disassembly and facilitates attacks to microbial cell membranes. In this work, we demonstrated additive effect of chitosan–PVP–TiO_2 ternary nanocomposite dressing with improved antibacterial, compatible with cell lines, good hydrophilic behavior and faster healing effect than control for wound healing applications.

2. Experimental

2.1. Materials

Chitosan (79% deacetylated) was purchased from Central Institute of Fisheries Technology (CIFT, Cochin, India). PVP was purchased from Central Drug House Pvt. Ltd., Mumbai, India. Nutrient agar and nutrient broth were obtained from Himedia, Mumbai, India. The test strains *Escherichia coli* (MTCC 739, Gram +ve), *Staphylococcus aureus* (MTCC 3160, Gram +ve), *Pseudomonas aeruginosa* (MTCC 1688, Gram −ve) and *Bacillus subtilis* (MTCC 121, Gram +ve) were obtained from IMTECH, Chandigarh, India. Double distilled water was used as solvent throughout the experiment.

2.2. Preparation of TiO_2 nanorod powder

0.001 mol titanium and 0.05 mol ammonium chloride powders were mixed and grounded in a carnelian mortar, then transferred to a corundum crucible. The crucible containing the mixture was heated at 600 °C for 3 h in an electric oven and then allowed to cool to room temperature naturally. The resultant solid powder was directly collected as the final product.

2.3. Preparation of chitosan–PVP–TiO_2 ternary nanocomposite dressing

Chitosan powder was first dissolved in 1% acetic acid solution and then added to PVP solution. To the above mixture, 10 mg of titanium dioxide nanorod powder was added and continuously stirred to form homogeneous mixture. The gel-like solution was poured onto ceramic plate in a dust free environment and dried in air at room temperature for 48 h and then in vacuum oven to obtain dry composite dressing.

2.4. Characterization of chitosan nanocomposite dressing

The infrared spectra were recorded on Perkin Elmer RX1 FTIR spectrophotometer. The morphology was studied by JEOL JSM-5200 model scanning electron microscopy at 15 kV. TGA was carried out at Perkin Elmer diamond analyzer. The size distribution of the TiO_2 nanoparticles was measured using a transmission electron microscope and scanning electron microscope. The mechanical properties of the films were determined by using a universal testing machine (Model 1185, Instron, USA) with a crosshead speed of 5 mm/min under 10 Hz at 23 °C. Dressing's thickness (mm) was determined on six films per ratio treatment averaging measurements at five points for each film using a screw gauge and verified with Vernier caliper.

2.5. Swelling test

The prepared chitosan–PVP–titanium dioxide based dressings were immersed in phosphate buffer saline (PBS) (pH 7.4) solution for different times at room temperature. Excess surface water was blotted out with filter paper before weighing. The procedure was repeated until there was no further weight increase. Percentage swelling of ternary film at equilibrium was calculated from the formula (Dhimana, Ray, & Panda, 2004)

$$\mathrm{DS} = \left[\frac{W_w - W_d}{W_d}\right] \times 100$$

where DS is the degree of swelling, W_w and W_d are weights of wet and dry film, respectively.

2.6. Water vapor transmission rate

Water absorption studies are of great importance for a biodegradable material. Water vapor transmission (WVT) of films was determined gravimetrically at 25 °C to find the moisture barrier properties of free films at room temperature and also their tightness and homogeneity. Free dressings with appropriate dimensions were sealed to WVT cups containing 10 ml of distilled water. The cups were accurately weighed and placed in a desiccator containing silica gel and appropriate amounts of calcium chloride to create a climate of low relative humidity (approximately 0%). Then, the cups were re-weighed at determined intervals (24, 48, 72, 96 and 120 h) and the profile of mass change *versus* time was plotted for each free dressing. WVTR was calculated using following equation:

$$\mathrm{WVTR}\ \ (\mathrm{g^{-2}\,day^{-1}}) = \left[\frac{g \times 27}{tA}\right]$$

where g represents mass loss, t is time (measured in hours during which the weight loss occurred), and A is the exposed area of the dressing (Mooter, Samyn, & Kinget, 1994).

2.7. In vitro antibacterial test

Antimicrobial test was performed using agar disc diffusion method (Tripathi et al., 2009a, 2009b). The agar diffusion test is a method commonly used to examine antimicrobial activity regarding the diffusion of the compound tested through water-containing agar plate (Singh & Dutta, 2010). For antibacterial activity nutrient agar (2.8 g in 100 ml water), nutrient broth (1.3 g in 100 ml water) were prepared and sterilized. The nutrient agar media was then poured into autoclaved petri dishes. A loopful of each bacterial strain was spread on nutrient agar and incubated at 37 °C for 24 h to give single colonies. A representative bacteria colony was picked off with a wire loop, placed in pre-sterilized nutrient broth and then incubated overnight at 37 °C for 12 h. By appropriately diluting with sterile distilled water and nutrient broth, the cultures of bacteria containing $\sim 10^8$ CFU/ml were prepared. Then prepared bacteria medium was dispensed on to agar plate and the solution was placed. The incubation was continued for 12 h at 37 °C inhibition zone was measured.

2.8. Blood compatibility assay

2.8.1. Blood collection

Approximately 50 ml whole blood was drawn from healthy volunteers into syringes preloaded with 10% acid citrate dextrose (ACD). ACD solution was prepared by mixing 0.544 g anhydrous citric acid, 1.65 g trisodium citrate dihydrate and 1.84 g dextrose monohydrate with 75 ml distilled water (Qu, Wu, & Chen, 2006). The first milliliter of ACD was discarded.

2.8.2. Hemolysis assay

Blood testing solution was prepared by diluting 4 ml fresh ACD human blood with 5 ml 0.9% saline. Dressing was cut into small pieces (approximately 1 cm × 1 cm) and equilibrated in 4 ml saline for 30 min at 37 °C. Diluted blood (0.2 ml) was added to each sample and incubated for 60 min at 37 °C. Positive or negative controls, which did not contain material films, were performed by adding 0.2 ml of human blood to 4.0 ml of distilled water (100% hemolysis) or saline solution (0% hemolysis), respectively. All solutions were centrifuged at 1000 rpm for 5 min. The absorbance of the supernatant was measured at 545 nm. Hemolysis was calculated as described by Dey and Ray (2003) as follows:

$$\text{Hemolysis}\ \ (\%) = \left[\frac{\text{OD}_{\text{test}} - W_{\text{neg}}}{\text{OD}_{\text{pos}} - \text{OD}_{\text{neg}}}\right] \times 100$$

In this equation, OD_{neg} control is the adsorption of 0.2 ml human blood dissolved in 4 ml distilled saline solution; OD_{pos} control is the adsorption of 0.2 ml human blood dissolved in 4 ml water; OD_{test} is the absorption of sample. All the hemolysis experiments were performed in triplicate.

2.9. Cell culture

Two cell lines, L929 and NIH3T3 (mouse fibroblast and embryonic cell lines, respectively, NCCS, Pune, India) were used in this study. For the cytotoxicity test, NIH3T3 and L929 cells were cultured in minimum essential medium (MEM) supplemented with 10% fetal bovine serum (FBS), 50 IU ml^{-1} penicillin, 50 μg ml^{-1} streptomycin (Invitrogen, CA, USA). NIH3T3 and L929 cells were seeded in to 96 well plates at a seeding density 1×10^4 cells/well and incubated for overnight.

2.10. Cytotoxicity test

Cell viability of the prepared samples was evaluated by indirect cytotoxicity test using Alamar blue (Kumar et al., 2010). The cytotoxicity test of samples was done according to ISO 10993-5. The cytotoxic effect of samples was evaluated on NIH3T3 (Li, Kong, et al., 2012; Li, Nan, et al., 2012) and L929 cells (Kim et al., 2004). Samples were sterilized by ethylene oxide gas treatment with 50 mg/ml (sample/medium) extraction ratio. Triplicates of each sample were taken and incubated in serum containing media for 24 h at 37 °C. 100 μl of the media from each sample was taken and transferred into each well. The cells were then incubated for 1, 3 and 7 days using Alamar blue assay (Invitrogen, USA). The optical density was measured at 570 nm with 620 nm set as the reference wavelength using a microplate spectrophotometer (Biotek Power Wave XS, USA).

2.11. In vivo wound healing study

Wound closure rate was evaluated using albino rat model. The animal study was carried out abiding by the national regulations related to the conduct of experimentation. Adult male albino rats (140–180 g) were used in the present study. The mice were divided into four treatment groups: gauze (negative control), soframycin skin ointment (positive control), chitosan, nanocomposite dressing; each group contained six rats (total 24 rats). The animals were anesthetized with an intraperitoneal (i.p.) injection of pentobarbitone sodium (50 mg/kg). A 2 cm × 2 cm (400 mm^2) open excision-type wound was created to the depth of loose subcutaneous tissue. Animals after recovery from anesthesia were housed individually in properly disinfected cages at room temperature of 25 ± 2 °C. During this period, the animals were repeatedly and gently handled to minimize the stress and to get them acclimatized to the laboratory environment.

On 0th, 7th, 11th and 16th postoperative days, the dressings were removed and the appearance of the wound was photographed. The rate of wound closure was determined by the following equation:

$$\text{Wound area} = \left[\frac{A_t}{A_0}\right] \times 100$$

where A_t and A_0 were the wound areas on the specified day and the day of operation, respectively.

2.12. Statistical analysis

All experimental values are presented as means ± S.D. The data were analyzed using ANOVA, and then Tukey's test was used to analyze multiple differences between the groups by using OriginPro software, version 8. p value at less than 0.05 was considered statistically significant.

3. Results and discussion

3.1. Characterization of chitosan nanocomposite dressing

3.1.1. Fourier transform infrared (FTIR) spectroscopy

The infrared spectra of chitosan and chitosan–PVP–TiO_2 films are depicted in Fig. 1. For chitosan spectrum (Fig. 1(a)): 3422 cm^{-1} (O—H stretch overlapped with N—H stretching), 2921 and 2867 cm^{-1} (C—H stretch), 2364 cm^{-1} (C—N asymmetric band stretching), 1653 cm^{-1} (amide II band, C—O stretch of acetyl group), 1592 cm^{-1} (amide II band, N—H stretch), 1375 cm^{-1} (asymmetric C—H bending of CH_2 group) and 1071 cm^{-1} (skeletal vibration involving the bridge C—O stretch) of glucosamine residue (Singh

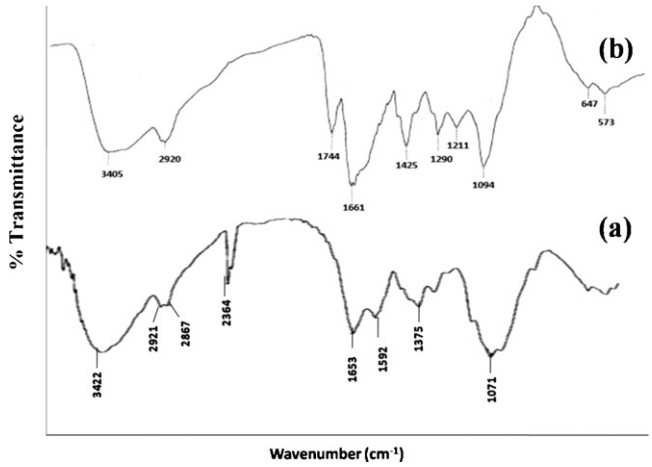

Fig. 1. FTIR spectra of chitosan (a), chitosan–PVP–TiO_2 nano dressing material (b).

et al., 2009). The IR spectrum of chitosan–PVP–TiO_2 nanocomposite dressing (Fig. 1(b)) contains the characteristic adsorption bands of the two polymer components. The —OH band in chitosan appears at 3422 cm^{-1} where as in composite dressing appears at 3405 cm^{-1}. This shifting of peak toward lower frequency range is due to hydrogen bonding between —OH of PVP and —OH or —NH_2 of chitosan (Wang, Liu, et al., 2012; Wang, Wang, et al., 2012; Wang, Zhu, et al., 2012). PVP and chitosan can form a homogeneous phase due to the strong hydrogen binding forces between two kinds of molecules (Anjali Devi, Smitha, Sridhar, & Aminabhavi, 2006).

3.1.2. Thermogravimetric analysis (TGA)

Thermal behavior of the chitosan and chitosan–PVP–TiO_2 dressing was investigated by TGA. TGA is considered as the most important method for studying thermal stability of polymers. Two weight losses are observed in the chitosan TGA curve shown in Fig. 2. The weight loss at 50–150 °C is due to the moisture vaporization. The other weight loss at 200–300 °C is due to the degradation of chitosan molecule. For nanocomposite dressing weight loss at 65–140 °C with a weight loss of 12% is due to loss of water. The second stage starts at 170–370 °C with a weight loss of 47.5% due to the decomposition (thermal and oxidative) of chitosan and PVP. The third stage starts at 400–500 °C with a weight loss of 11% due to grafting of nano titanium dioxide into chitosan PVP matrix.

3.1.3. Scanning electron microscopy (SEM) and transmission electron microscope (TEM)

Electron micrographs of SEM and TEM are used to evaluate the distribution of TiO_2 nanoparticles in chitosan–PVP matrix with its

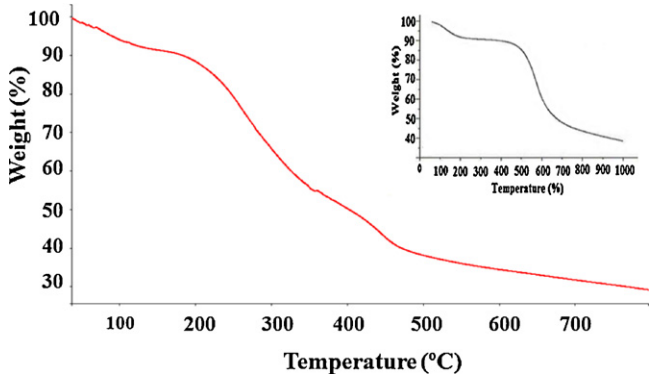

Fig. 2. TGA curve of chitosan–PVP–TiO_2 dressing material (inset chitosan thermogram).

morphological and crystallographic features. In Fig. 3(a) and (b) SEM exhibits the agglomerated distribution of TiO_2 nanoparticles in ternary matrix composition. The possibility of agglomeration could be due to the viscous nature of chitosan–PVP complex matrix that does not allow the TiO_2 nanoparticles to distribute uniformly in the whole binary polymer mixture under ambient stirring conditions. To alleviate the concern of agglomeration, sonication process could be a solution but its effect on the ternary composition is little understood and therefore avoided in this case. TEM studies (Fig. 3(c)) have shown spherical particles with good polycrystalline nature as shown by electron diffraction pattern (in inset). This diffraction pattern has close similarity with X-ray diffraction intensities (data not shown here). Fig. 3(d) demonstrates the histogram of TiO_2 nanoparticles embedded in binary polymer matrix that have shown average particle size of nanoparticles under consideration of about 25–35 nm with a good distribution for short ranges.

3.2. Swelling test

To prevent a secondary infection of bacteria, an ideal wound dressing absorbs wound fluid (Lin, Chen, & Chu, 2001). Water uptake ability of a biomaterial is an important factor for cell seeding, which affects distribution of cell suspension throughout the material and a transfer efficiency of oxygen and nutrient. The degree of swelling of the dressing determined through this investigation was calculated by applying conventional Flory Huggins swelling formula. There are several parameters affecting the swelling ratio, hydrophilicity, stiffness and pore structure of a matrix. The sample with the highest degree of swelling will have the highest surface area/volume ratio. The hydrophilic nature of chitosan material may be a major factor that influences the extent of swelling of these matrices. It can be easily observed from Fig. 4 that the film attains equilibrium state after certain period of time. The dressing shows the maximum swelling rate about 2289% after 6 h. This high swelling property of chitosan–PVP–TiO_2 dressing material is due to hydrophilic nature of material and important for quick absorption of exudates for wound healing materials.

3.3. Water vapor transmission rate

An ideal dressing should maintain evaporative water loss from the skin at an optimal rate. Queen et al. reported that a water vapor transmission rate of 2000–2500 g^{-2} day^{-1} would provide an adequate level of moisture to prevent excessive dehydration and build up the exudates on the wound area. A higher WVTR dried the wound more quickly and produces scars. Moreover, a lower WVTR accumulated exudates, which might retard the healing process and result in increased risk of bacterial growth (Queen, Gaylor, Evans, Courtney, & Reid, 1987). The WVTR of the nano ternary dressing material was 1950–2050 g^{-2} day^{-1} which is very close to the ideal value for wound dressing. According to Queen's recommendation, it seemed that nano ternary film is quite suitable as dressing material in terms of WVTRs.

3.4. Mechanical properties

To investigate the influence of chitosan on the mechanical properties of dressing material, their tensile strength (MPa) was evaluated. Tensile strength expresses the maximum stress developed in a film during tensile testing. Fig. 4(b) shows the effect of chitosan, PVP and nanoparticles on tensile strength of nanocomposite dressing. The tensile strength of chitosan, PVP with nanoparticle (1:1)* was maximum followed by chitosan, PVP without nanoparticle (1:1), chitosan, PVP (1:2) and chitosan, PVP (1:4) blended films. It was found that with a decreasing ratio of PVP up to 50% in the composite membranes, the strength of the prepared

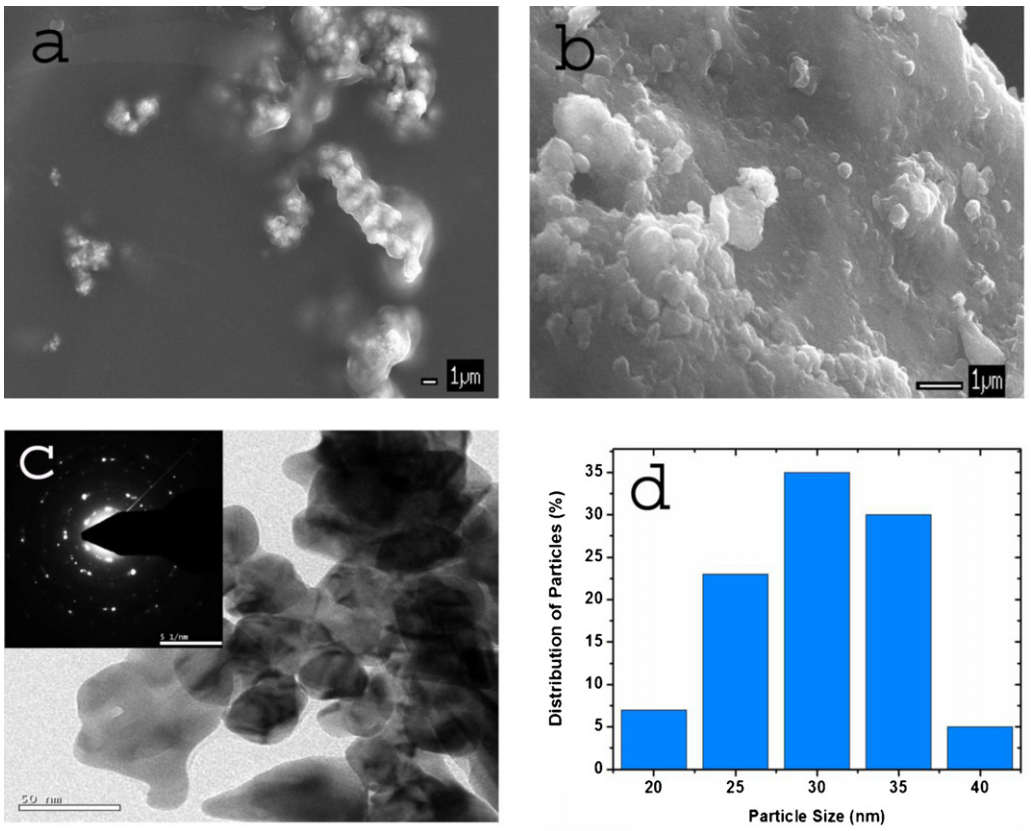

Fig. 3. Microscopic images of the chitosan–PVP–TiO_2 dressing material: scanning electron micrograph depicting a homogenous dispersion of titanium dioxide nanoparticles (scale 11 mm) (a, b), TEM of composite dressing material (scale 50 nm) (c) and histogram revealing the nanoparticle size distribution (d).

dressing significantly increased (Demirci, Alaslan, & Caykara, 2009). There were significant differences in tensile strength of without and with nanoparticle, demonstrating that the incorporation of nanoparticles modified the resistance of the dressing material. The tensile strength of chitosan–PVP–TiO_2 matrix without nanoparticle was 34.6 ± 1.0 MPa increasing to a maximum value of 36.28 ± 1.0 MPa when the nanoparticle was incorporated in composite dressing. For an ideal wound dressing material, the prepared nanocomposite film must have good tensile strength because the dressing should not be damaged by handling. From the study, it was found that 1:1 ratio of chitosan, PVP blended dressing with nanoparticle showed moderate tensile strength.

3.5. Antibacterial activity

Antimicrobial activity is the prerequisite condition for any wound dressing material because microbial contamination is a major cause of worry during treatment. Inhibitory effect of chitosan–PVP–TiO_2 ternary solution against microbial strains *E. coli*, *S. aureus*, *P. aeruginosa*, and *B. subtilis* are shown in Fig. 5. The inhibitory effect was measured based on clear zone surrounding circular film strips. Measurement of clear zone diameter included diameter of film strips, therefore, the values were always higher than the diameter of film strips whenever clearing zone was present. If there is no clear zone surrounding, we assumed

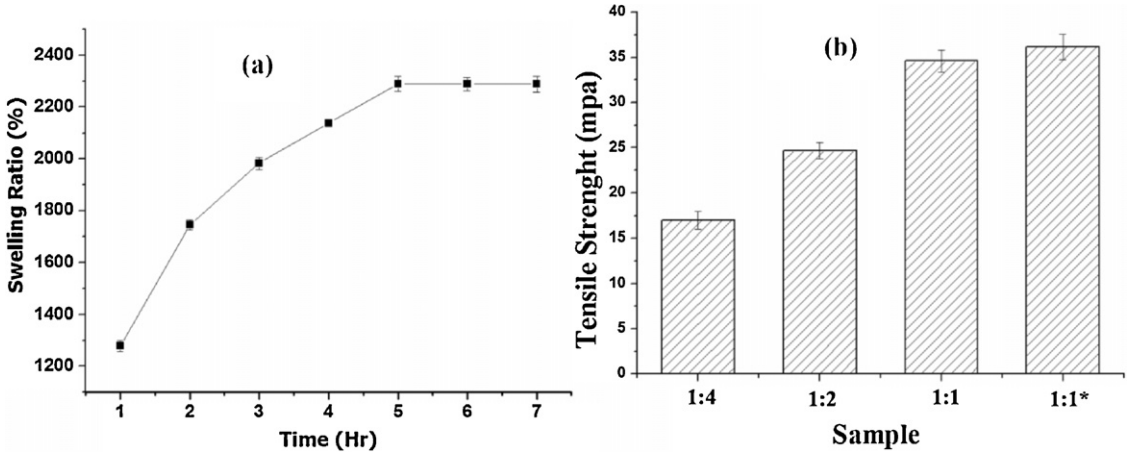

Fig. 4. Swelling studies of prepared dressing (a) and tensile strength of chitosan, PVP and TiO_2 blended dressing materials (b).

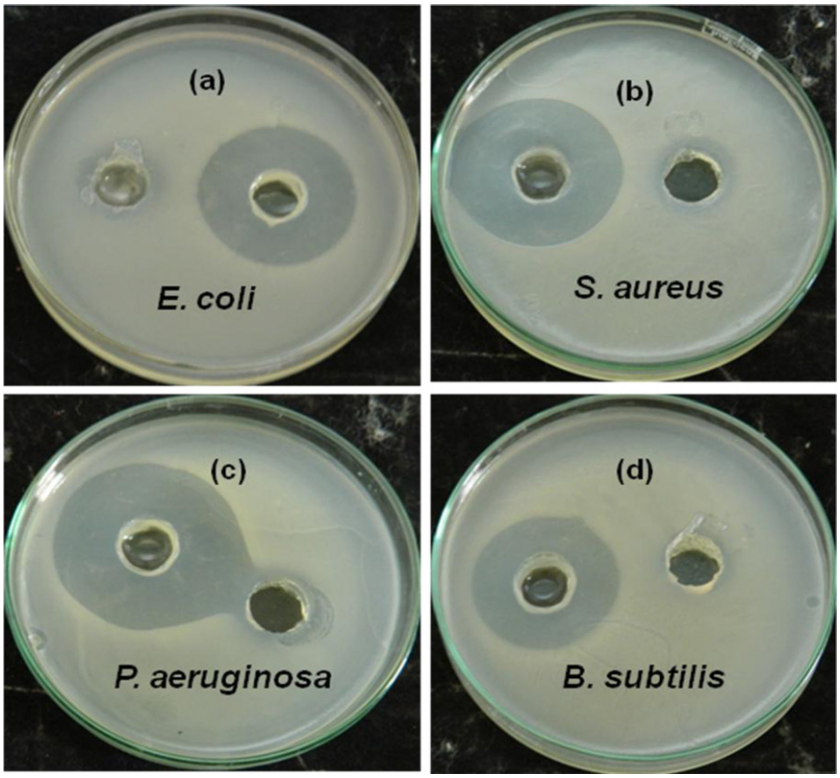

Fig. 5. Inhibitory effect of chitosan–PVP–TiO_2 solution against *E. coli* (a), *Staphylococcus aureus* (b), *Pseudomonas aeruginosa* (c) and *Bacillus subtilis* (d).

that there is no inhibitory zone, and furthermore, the diameter was valued as zero. The Antibacterial inhibition zone for chitosan–PVP–TiO_2 solution against different microbial strains, *i.e. E. coli* (Fig. 5(a)), *S. aureus* (Fig. 5(b)), *P. aeruginosa* (Fig. 5(c)), and *B. subtilis* (Fig. 5(d)) was measured as 30 mm, 32 mm, 38 mm and 28 mm, respectively. This inhibition zone against different microbial cultures proves that chitosan–PVP–TiO_2 dressing had an excellent antibacterial activity. Moreover, the antibiotic property of the nanocomposites against the gram positive was much more pronounced than against the gram negative. It is clear from the experiment that Gram-positive bacteria exhibited the most susceptibility to the nanocomposites in comparison to gram negative. This is due to nanocomposites may be a result of their cell wall plasmolysis or the separation of cytoplasm from their cell wall (Nathanael, Lee, Mangalaraj, Hong, & Rhee, 2012). The extremely high surface area of nanoscaled TiO_2 facilitated the adsorption of target bacteria, which accelerated the rate of antibacterial reaction (Kanna & Wongnawa, 2008).

3.6. Hemocompatibility

Hemolysis is considered to be a very simple and reliable measure of estimating blood compatibility of materials. Generally the smaller the Hemolysis value, the better the blood compatibility of the biomaterial. Autian, Kronenthal, Oser, and Martin (1975) reported that a value of up to 5% hemolysis is permissible for biomaterials. The nanocomposite dressing material induced 1.14% of contacting erythrocytes to hemolyze over 60 min of contact with whole blood. This is well within the permissible limit set by Autian. So prepared nano ternary dressing material could be considered highly hemocompatible.

3.7. Cytotoxicity test

The evaluation of cytotoxicity is very important for films used in wound healing applications. The biosafety and biocompatibility of chitosan–PVP (Wang, Liu, et al., 2012; Wang, Wang, et al., 2012; Wang, Zhu, et al., 2012) and nanosize TiO_2 materials had been previously studied by both *in vitro* and *in vivo* tests (Gulati et al., 2012; Li et al., 2007; Long, Saleh, Tilton, Lowry, & Veronesi, 2006).

The impact of the chitosan–PVP–TiO_2 dressing material on cell viability was assessed in two cell lines, L929 mouse fibroblast cells and NIH3T3 mouse embryonic cells using Alamar blue assay. In this study, the viability assay was measured for 1, 3 and 7 days after cell seeding, which is shown in Fig. 6. According to GB/T 16886.5-2003 (ISO 10993-5: 1999), samples with cell viability larger than 75% can be considered as noncytotoxic. Fig. 6(a) indicates that the cell viability is 98% after 3 days and 97% after7 days on NIH3T3 cells and for L929 (Fig. 6(b)) it is 97% after 3 days and 96% after seven days. The Alamar blue assay indicates that the cells grew very well after 7 days of exposure to ternary nanocomposite dressing material. Therefore, ternary film can be considered as biocompatible product.

Soto et al. have also done a correlation study between particle size, aggregation and toxicology using cellular experimental protocols. In these studies TEM is extensively used to analyze the particle sizes and the results suggest that TiO_2 are much less cytotoxic compared to other types of nanomaterials such as carbon nanotubes and SiO_2 (Soto, Carrasco, Powell, Garza, & Murr, 2005; Soto, Garza, & Murr, 2007). Yoshida et al. have reported that LDH (lactate dehydrogenase) assay revealed TiO_2 to be the least toxic material from sub-100 nm up to 1 mm. According to their studies toxicology assessed using cell membrane damage assays, metal oxides are toxic in the following order: $TiO_2 < Al_2O_3 < SiO_2$ regardless of size under 1 mm. This study, however, does not probe different types of TiO_2 (Yoshida, Morita, & Mishina, 2003).

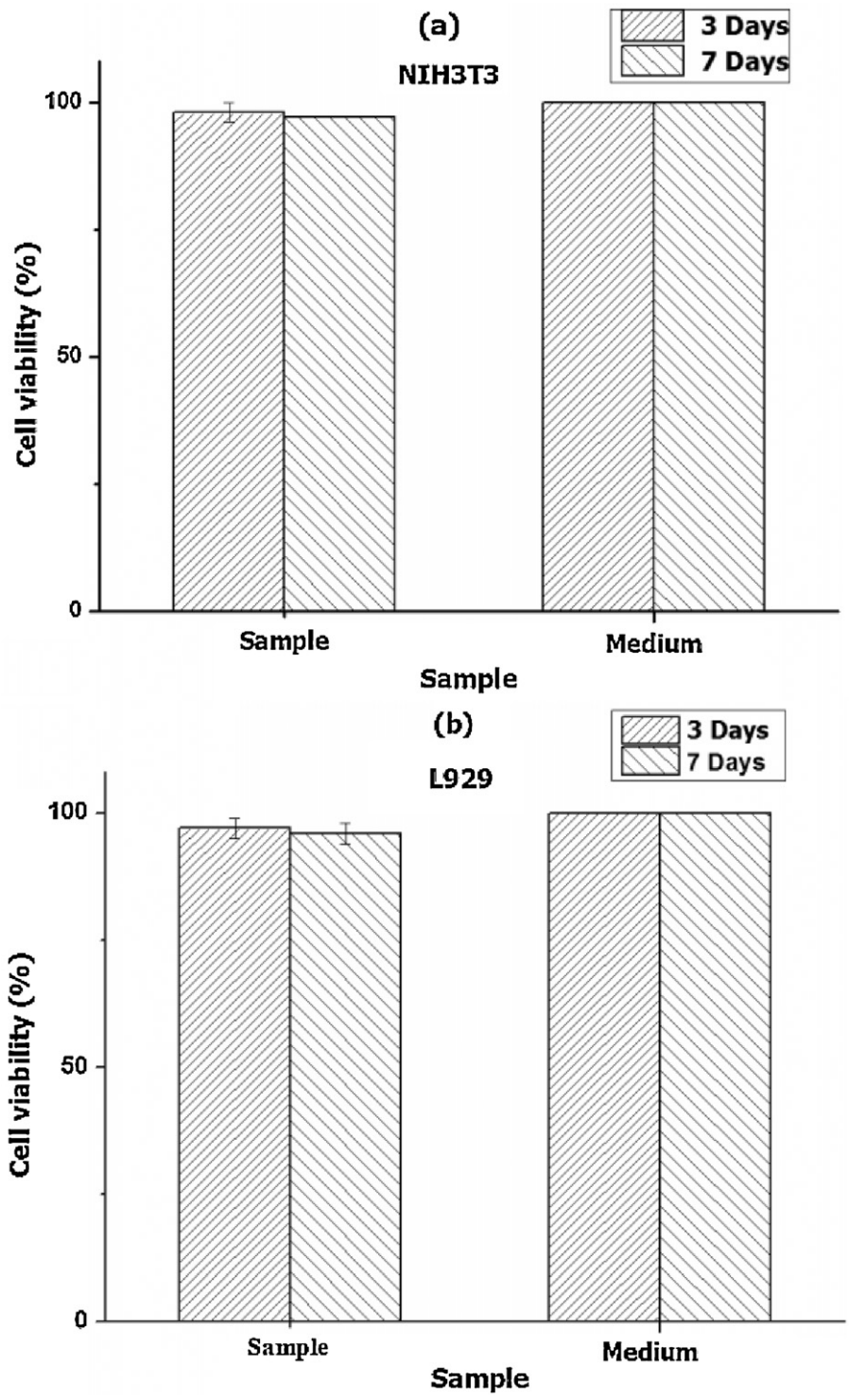

Fig. 6. Cytotoxicity profile of chitosan–PVP–TiO_2 dressing material in NIH3T3 (a) and L929 cells (b).

3.8. Photographic analysis

Representative images of each group, namely, negative control, positive control, chitosan and chitosan–PVP–TiO_2 dressing material onto Adult male albino rats and complete schematic functioning presentation of wound dressing material are shown in Fig. 7. At the day of surgery, no visible difference in wound appearance was observed for all groups. At the 7th day of post-surgery, granulation tissue formation was clearly observed in chitosan and chitosan–PVP–TiO_2 treated groups. On day 16, wounds treated with the chitosan–PVP–TiO_2, complete wound closure was observed. During the wound healing process, chitosan gradually depolymerizes to release N-acetylglucosamine, which initiates fibroblast proliferation and helps in ordered collagen deposition and stimulates increased level of natural hyaluronic acid synthesis at the wound site (Jayakumar, Prabaharan, Kumar, Nair, & Tamura, 2011). Nho and Park (2002) reported that the PVA/PVP–chitosan hydrogel dressing stopped the bleeding from the wound and had a better

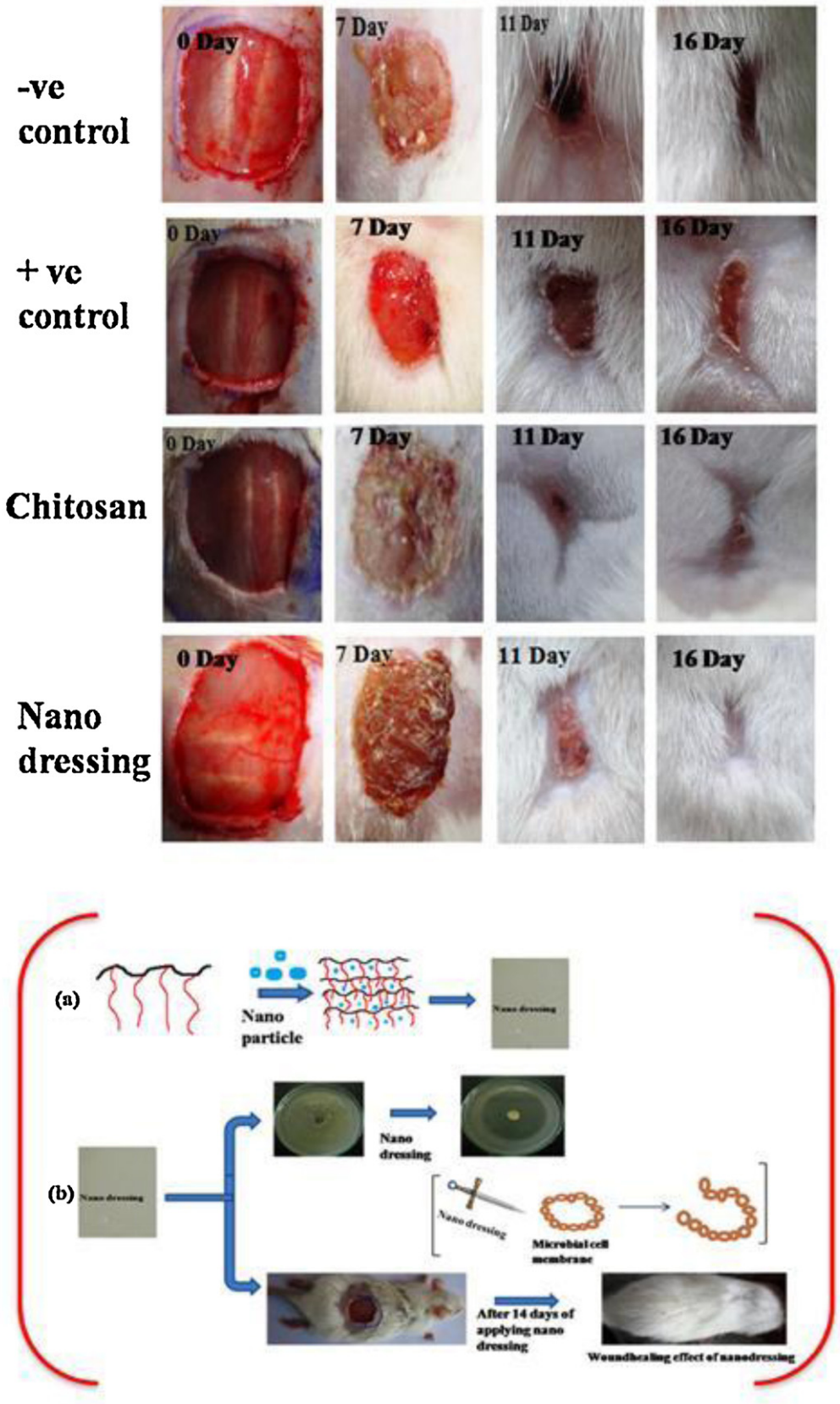

Fig. 7. *In vivo* study of wounds onto Adult male albino rats (140–180 g) and complete schematic functioning presentation of wound dressing material.

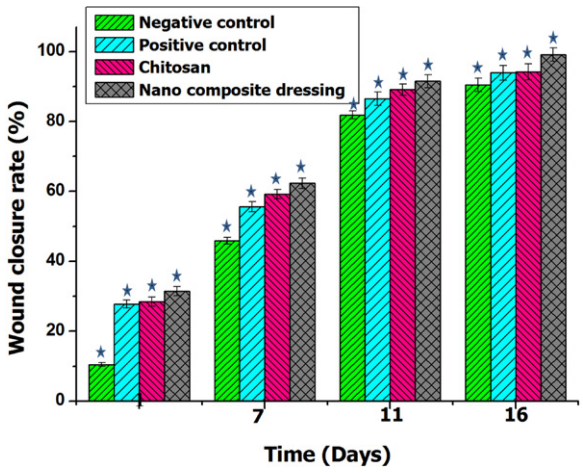

Fig. 8. Wound closure profiles of the wounds treated with negative control, positive control, chitosan and nano dressing. The data are presented with mean ± S.D. ($N = 6$). The star (⋆) indicate a significant difference at $p < 0.05$.

curing effect than the vaseline gauze. The nanoparticles provide a slow release of titanium ions that have wound healing and antimicrobial properties. The titanium ions released from nanoparticle inhibits microbial proliferation and hence it accelerates wound healing during *in vivo* test (Lipovsky, Gedanken, Nitzan, & Lubart, 2011).

3.9. Wound closure observation

Many researchers demonstrated preparation of nanocomposites based on chitosan for wound healing applications. Lu, Gao, and Gu (2008) fabricated wound dressing composed of nano-Ag and chitosan to observe the healing rate of Ag-chitosan dressing. The rate of nano dressing with healing time of 13.51 ± 4.56 days was higher (99%) than control Ag sulfadiazine with 17.45 ± 6.23 days (82%). The affects of wound environment for nano-Ag was far less than the ionic form of Ag, in the same concentration, and this is due to the bactericidal activity of nano-Ag is greater than that of the ionic form of Ag. Lu et al. (2010) also reported that gold colloid/chitosan scaffold could promote adhesion and proliferation of keratinocytes. Kumar et al. (2012) prepared microporous chitosan hydrogel/nano ZnO composite bandages (CZBs) for wound dressing applications. In this study after two weeks, the CZBs achieved significant closure to 90% only assisted by the chitosan control and comparison to Kaltostat-treated wound and bare wounds (70%). Peng et al. (2008) prepared TiO_2–chitosan with collagen nanocomposite (NTCAS) for artificial skin. In the animal model, NTCAS showed better and faster recovery than the other groups, which can be attributed to the unique bactericidal effect of nano-TiO_2 and immune-enhancing effect of chitosan. Commercialization of these new nanoparticles based wound dressing materials (Ulkur, Oncul, Karagoz, Yeniz, & Celikoz, 2005) is sprouting almost as fast as they are developed.

In our investigation, the wounds treated with chitosan–PVP–TiO_2 dressing material healed faster than chitosan and those of the control groups. Fig. 8 shows the wound closure rate (WCR, %) of +ve control, −ve control, pure chitosan and chitosan–PVP–TiO_2 matrices. All experimental groups began to show reductions in open wound area from day 3. The wound closure rate of the negative control group is 10.45%, 45.91%, 81.87%, and 90.42% for 3, 7, 11 and 16 days, respectively. The wound closure rate of the positive control group is 27.79%, 55.58%, 86.51%, and 93.34% for 3, 7, 11 and 16 days, respectively. The wound closure rate of the chitosan treated group is 28.48%, 59.19%, 89.11%, and 94.21% for 3, 7, 11 and 16 days, respectively. The wound closure rate of the chitosan–PVP–TiO_2 treated group is 31.48%, 62.33%, 91.49%, and 99.09% for 3, 7, 11 and 16 days, respectively which is more than CZBs as reported by Kumar et al. (2012). The prepared dressings neither dissolve during the application period nor adhere to the wound and were easy to remove without ripping the skin.

On day 16, the wounds treated with the chitosan–PVP–TiO_2 nanocomposite film had healed almost completely (99%), whereas in chitosan, negative control and positive control treated groups the wound closure rates are 94%, 90% and 93%, respectively. Finally, wounds healed under the chitosan–PVP–TiO_2 sheet *via in vivo* test demonstrated better tissue quality with less scarring.

4. Conclusion

In conclusion, a new dressing consisting of biopolymer chitosan, synthetic polymer poly(N-vinylpyrrolidone) (PVP) and nanoparticle titanium dioxide has been developed, which had powerful antibacterial efficacy against four pathogenic bacteria and found nontoxic toward NIH3T3 and L929 fibroblast cells. In full-thickness wound model of albino rats, the wound closure rate is effective in nanocomposite treated wounds compared with that treated with chitosan, positive control and negative control groups. From the outcome of the *in vivo* evaluation, it is concluded that the reported nanocomposite film is effective for wound care.

References

Altemeier, W. A., Schiff, L., Gall, E. A., Giuseffi, J., Freiman, D., Mindrum, G., et al. (1954). Physiological and pathological effects of long-term polyvinylpyrrolidone retention. *American Medical Association Archives of Surgery*, *69*, 309–314.

Amiji, M. M. (1995). Permeability and blood compatibility properties of chitosan–poly(ethylene oxide) blend membranes for haemodialysis. *Biomaterials*, *16*, 593–599.

Anjali Devi, D., Smitha, B., Sridhar, S., & Aminabhavi, T. M. (2006). Novel crosslinked chitosan/poly(vinylpyrrolidone) blend membranes for dehydrating tetrahydrofuran by the pervaporation technique. *Journal of Membrane Science*, *280*, 45–53.

Archana, D., Dutta, J., & Dutta, P. K. (2010). Chitosan–pectin–titanium dioxide nanocomposite film: An investigation for wound healing applications. *Asian Chitin Journal*, *6*, 45–46.

Autian, J., Kronenthal, R. L., Oser, Z., & Martin, E. (1975). Biological model systems for the testing of the toxicity of biomaterials. In *Polymer science and technology, vol. 8: Polymers in medicine and surgery*. New York: Plenum Press., p. 181.

Brammer, K. S., Oh, S., Gallagher, J. O., & Jin, S. (2008). Enhanced cellular mobility guided by TiO_2 nanotube surfaces. *Nano Letters*, *8*, 786–793.

Chen, Y., Yan, L., Yuan, T., Zhang, Q., & Fan, H. (2011). Asymmetric polyurethane membrane with in situ-generated nano-TiO_2 as wound dressing. *Journal of Applied Polymer Science*, *119*, 1532–1541.

Demirci, S., Alaslan, A., & Caykara, T. (2009). Preparation, characterization and surface pK_a values of poly(N-vinyl-2-pyrrolidone)/chitosan blend films. *Applied Surface Science*, *255*, 5979–5983.

Dey, R. K., & Ray, A. R. (2003). Synthesis, characterization, and blood compatibility of polyamidoamines copolymers. *Biomaterials*, *24*, 2985–2993.

Dhimana, H. K., Ray, A. R., & Panda, A. K. (2004). Characterization and evaluation of chitosan matrix for in vitro growth of MCF-7 breast cancer cell lines. *Biomaterials*, *25*, 5147–5154.

Grassian, V. H., Oshaughnessy, P. T., Adamcakova-Dodd, A., Pettibone, J. M., & Thorne, P. S. (2007). Inhalation exposure study of titanium dioxide nanoparticles with a primary particle size of 2 to 5 nm. *Environmental Health Perspectives*, *115*, 397–402.

Gulati, K., Ramakrishnan, S., Sinn, M. A., Atkins, G. J., Findlay, D. M., & Losic, D. (2012). Biocompatible polymer coating of titania nanotube arrays for improved drug elution and osteoblast adhesion. *Acta Biomaterialia*, *8*, 449–456.

Han, J. B., Su, H. J., & Tan, T. W. (2006). Study on sterilizing action on *E. coli* of nano-TiO_2–chitosan multiplex dressing material. *New Chemical Materials*, *34*, 65–68.

Hong, Y., Chirila, T. V., Vijayasekaran, S., Shen, W., Lou, X., & Dalton, P. (1998). Biodegradation in vitro and retension in the rabbit eye of crosslinked poly(1-vinyl-2-pyrrilidone) hydrogel as vitreous substitute. *Journal of Biomedical Materials Research*, *39*, 650–659.

Ian, T., Su, H., & Tan, T. (2011). The bactericidal and mildew-proof activity of a TiO_2–chitosan composite. *Journal of Photochemistry and Photobiology A*, *218*, 130–136.

Jayakumar, R., Prabaharan, M., Kumar, S. P. T., Nair, S. V., & Tamura, H. (2011). Biomaterials based on chitin and chitosan in wound dressing applications. *Biotechnology Advances*, *29*, 322–337.

Jayakumar, R., Selvamurugan, N., Nair, S. V., Tokura, S., & Tamura, H. (2008). Preparative methods of phosphorylated chitin and chitosan – An overview. *International Journal of Biological Macromolecules*, *43*, 221–225.

Jia, Y., Hu, Y., Zhu, Y., Che, L., Shen, Q., Zhang, J., et al. (2011). Oligoamines conjugated chitosan derivatives: Synthesis, characterization, *in vitro* and *in vivo* biocompatibility evaluations. *Carbohydrate Polymers*, *83*, 1153–1161.

Kanna, M., & Wongnawa, S. (2008). Mixed amorphous and nanocrystalline TiO_2 powders prepared by sol–gel method: Characterization and photocatalytic study. *Materials Chemistry and Physics*, *110*, 166–175.

Kean, T., Roth, S., & Thanou, M. (2005). Trimethylated chitosans as non-viral gene delivery vectors: Cytotoxicity and transfection efficiency. *Journal of Controlled Release*, *103*, 643–653.

Kim, J. H., Sim, S. J., Lee, D. H., Kim, D., Lee, Y. K., Chung, D. J., et al. (2004). Preparation and properties of PHEA/chitosan composite hydrogel. *Polymer Journal*, *36*, 943–948.

Kumar, P. T. S., Abhilash, S., Manzoor, K., Nair, S. V., Tamura, H., & Jayakumar, R. (2010). Preparation and characterization of novel b-chitin/nanosilver composite scaffolds for wound dressing applications. *Carbohydrate Polymers*, *80*, 761–767.

Kumar, P. T. S., Lakshmanan, V. K., Kumar, T. V. A., Ramya, C., Reshmi, P., Unnikrishnan, A. G., et al. (2012). Flexible and microporous chitosan hydrogel/nano ZnO composite bandages for wound dressing: In vitro and in vivo evaluation. *ACS Applied Materials & Interfaces*, *4*, 2618–2629.

Leea, Y. H., Chang, J. J., Yang, M. C., Chien, C. T., & Lai, W. F. (2012). Acceleration of wound healing in diabetic rats by layered hydrogel dressing. *Carbohydrate Polymers*, *88*, 809–819.

Li, J., Li, Q., Xu, J., Li, J., Cai, X., Liu, R., et al. (2007). Comparative study on the acute pulmonary toxicity induced by 3 and 20 nm TiO_2 primary particles in mice. *Environmental Toxicology and Pharmacology*, *24*, 239–244.

Li, X., Kong, X., Zhanga, Z., Nana, K., Li, L. L., Wang, X. H., et al. (2012). Cytotoxicity and biocompatibility evaluation of N,O-carboxymethyl chitosan/oxidized alginate hydrogel for drug delivery application. *International Journal of Biological Macromolecules*, *50*, 1299–1305.

Li, X., Nan, K., Li, L., Zhang, Z., & Chen, H. (2012). In vivo evaluation of curcumin nanoformulation loaded methoxy poly(ethylene glycol)-graft-chitosan composite film for wound healing application. *Carbohydrate Polymers*, *88*, 84–90.

Lu, S. Y., Gao, W. J., & Gu, H. Y. (2008). Construction, application and biosafety of silver nanocrystalline chitosan wound dressing. *Burns*, *34*, 623–628.

Lu, S. Y., Xia, D. L., Huang, G. J., Jing, H. X., Wang, Y. F., & Gu, H. Y. (2010). Concentration effect of gold nanoparticles on proliferation of keratinocytes. *Colloids and Surfaces B: Biointerfaces*, *81*, 406–411.

Lieder, R., Darai, M., Thor, M. B., Ng, C. H., Einarsson, J. M., Gudmundsson, S., et al. (2012). In vitro bioactivity of different degree of deacetylation chitosan, a potential coating material for titanium implants. *Journal of Biomedical Materials Research Part A*, *100*, 3392–3399.

Lipovsky, A., Gedanken, A., Nitzan, Y., & Lubart, R. (2011). Enhanced inactivation of bacteria by metal-oxide nanoparticles combined with visible light irradiation. *Lasers in Medical Science*, *43*, 236–240.

Lin, S. Y., Chen, K. S., & Chu, R. L. (2001). Design and evaluation of drug loaded wound dressing having thermo responsive, adhesive, absorptive, and easy peeling properties. *Biomaterials*, *22*, 2999–3004.

Long, T. C., Saleh, N., Tilton, R. D., Lowry, G. V., & Veronesi, B. (2006). Titanium dioxide (P25) produces reactive oxygen species in immortalized brain microglia (BV2): Implications for nanoparticle neurotoxicity. *Environmental Science and Technology*, *40*, 4346–4352.

Mooter, G. V. D., Samyn, C., & Kinget, R. (1994). Characterization of colon-specific azopolymers: A study of the swelling properties and permeability of isolated polymers dressing materials. *International Journal of Pharmaceutics*, *111*, 127–136.

Muzzarelli, R. A. A., Greco, F., Busilacchi, A., Sollazzo, V., & Gigante, A. (2012). Chitosan, hyaluronan and chondroitin sulfate in tissue engineering for cartilage regeneration: A review. *Carbohydrate Polymers*, *89*, 723–739.

Muzzarelli, R. A. A. (2009). Chitins and chitosans for the repair of wounded skin, nerve, cartilage and bone. *Carbohydrate Polymers*, *76*, 167–182.

Muzzarelli, R. A. A., Morganti, P., Morganti, G., Palombo, P., Palombo, M., Biagini, G., et al. (2007). Chitin nanofibrils/chitosan glycolate composites as wound medicaments. *Carbohydrate Polymers*, *70*, 274–284.

Nathanael, A. J., Lee, J. H., Mangalaraj, D., Hong, S. I., & Rhee, Y. H. (2012). Multifunctional properties of hydroxyapatite/titania bio-nano-composites: Bioactivity and antimicrobial studies. *Powder Technology*, *228*, 410–415.

Nho, Y. C., & Park, K. R. (2002). Preparation and properties of PVA/PVP hydrogels containing chitosan by radiation. *Journal of Applied Polymer Science*, *85*, 1787–1794.

Peng, C. C., Yang, M. H., Chiu, W. T., Chiu, C. H., Yang, C. S., Chen, Y. W., et al. (2008). Composite nano-titanium oxide–chitosan artificial skin exhibits strong wound-healing effect-an approach with anti-inflammatory and bactericidal kinetics. *Macromolecular Bioscience*, *8*, 316–327.

Peng, L., Eltgroth, M. L., LaTempa, T. J., Grimes, C. A., & Desai, T. A. (2009). The effect of TiO_2 nanotubes on endothelial function and smooth muscle proliferation. *Biomaterials*, *30*, 1268–1272.

Qu, X. H., Wu, Q., & Chen, G. Q. (2006). *In vitro* study on hemocompatibility and cytocompatibility of poly(3-hydroxybutyrate-*co*-3-hydroxyhexanoate). *Journal of Biomaterials Science, Polymer Edition*, *17*, 1107–1121.

Queen, D., Gaylor, J. D. S., Evans, J. H., Courtney, J. M., & Reid, W. H. (1987). The preclinical evaluation of the water vapor transmission rate through burn wound dressings. *Biomaterials*, *8*, 367–371.

Sayes, C. M., Wahi, R., Kurian, P. A., Liu, Y., West, J. L., Ausman, K. D., et al. (2006). Correlating nanoscale titania structure with toxicity: A cytotoxicity and inflammatory response study with human dermal fibroblasts and human lung epithelial cells. *Toxicology Science*, *92*, 174–185.

Singh, D. K., & Ray, A. (2000). Biomedical applications of chitin, chitosan and their derivatives. *Journal of Macromolecular Science, Part C: Polymer Reviews*, *40*, 69–83.

Singh, J., & Dutta, P. K. (2010). Preparation, antibacterial and physicochemical behavior of chitosan/ofloxacin complexes. *International Journal of Polymeric Materials*, *59*, 793–807.

Singh, J., Dutta, P. K., Dutta, J., Hunt, A. J., Macquarrie, D. J., & Clark, J. H. (2009). Preparation and properties of highly soluble chitosan–L-glutamic acid aerogel derivative. *Carbohydrate Polymers*, *76*, 188–195.

Soto, K. F., Carrasco, A., Powell, T. G., Garza, K. M., & Murr, L. E. (2005). Comparative in vitro cytotoxicity assessment of some manufactured nanoparticulate materials characterized by transmission electron microscopy. *Journal of Nanoparticle Research*, *7*, 145–169.

Soto, K., Garza, K. M., & Murr, L. E. (2007). Cytotoxic effects of aggregated nanomaterials. *Acta Biomaterialia*, *3*, 351–358.

Tang, C., Chen, N., Zhang, Q., Wang, K., Fu, Q., & Zhang, X. (2009). Preparation and properties of chitosan nanocomposites with nanofillers of different dimensions. *Polymer Degradation and Stability*, *9*, 124–131.

Tripathi, S., Mehrotra, G. K., & Dutta, P. K. (2009a). Preparation and physicochemical evaluation of chitosan/poly(vinyl alcohol)/pectin ternary film for food-packaging applications. *Carbohydrate Polymers*, *79*, 711–716.

Tripathi, S., Mehrotra, G. K., & Dutta, P. K. (2009b). Physicochemical and bioactivity of cross-linked chitosan–PVA film for food packaging applications. *International Journal of Biological Macromolecules*, *45*, 372–376.

Ulkur, E., Oncul, O., Karagoz, H., Yeniz, E., & Celikoz, B. (2005). Comparison of silver-coated dressing (Acticoat™), chlor hexidine acetate 0.5% (Bactigrass®), and fusidic acid 2% (Fucidin®) for topical antibacterial effect in methicillin-resistant Staphylococci-contaminated, full-skin thickness rat burn wounds. *Burns*, *31*, 874–877.

Wang, B. L., Liu, X. H., Ji, Y., Ren, B. F., & Ji, J. (2012). Fast and long-acting antibacterial properties of chitosan–Ag/polyvinylpyrrolidone nanocomposite films. *Carbohydrate Polymers*, *90*, 8–15.

Wang, B. L., Wang, J. L., Li, D. D., Ren, K. F., & Ji, J. (2012). Chitosan/poly(vinyl pyrollidone) coatings improve the antibacterial properties of poly(ethylene terephthalate). *Applied Surface Science*, *258*, 7801–7808.

Wang, T., Zhu, X. K., Xue, X. T., & Wu, D. Y. (2012). Hydrogel sheets of chitosan, honey and gelatin as burn wound dressings. *Carbohydrate Polymers*, *88*, 75–83.

Wist, J., Sanabria, J., Dierolf, C., Torres, W., & Pulgarin, C. (2004). Evaluation of photocatalytic disinfection of crude water for drinking water production. *Journal of Photochemistry and Photobiology A: Chemistry*, *147*, 241–246.

Yoshida, K., Morita, M., & Mishina, H. (2003). Cytotoxicity of metal and ceramic particles in different sizes. *JSME International Journal Series C, Mechanical Systems, Machine Elements and Manufacturing*, *46*, 1284–1289.

Zileinski, B. A., & Acbischer, P. (1994). Chitosan as a matrix for mammalian cell encapsulation. *Biomaterials*, *15*, 1049–1056.